



Published in final edited form as:

Ocul Surf. 2017 April ; 15(2): 193–201. doi:10.1016/j.jtos.2016.12.002.

Bulbar conjunctival microvascular responses in dry eye

Wan Chen, MD, PhD^{1,2}, Hatim Ismail M. Batawi, MD^{2,3}, Jimmy R. Alava, MD³, Anat Galor, MD, MSPH^{2,3}, Jin Yuan, MD, PhD^{1,2}, Constantine D. Sarantopoulos, MD, PhD^{3,4}, Allison L. McClellan, OD³, William J. Feuer, MS², Roy C. Levitt, MD^{3,4,5}, and Jianhua Wang, MD, PhD²

¹Zhongshan Ophthalmic Centre, Sun Yat-sen University, Guangzhou, Guangdong, China

²University of Miami Miller School of Medicine, Bascom Palmer Eye Institute, Miami, Florida

³Miami Veterans Administration Medical Center, Miami, Florida

⁴Department of Anesthesiology, Perioperative Medicine and Pain Management

⁵John T. Macdonald Foundation Department of Human Genetics, and the John P. Hussman Institute of Human Genomics, University of Miami Miller School of Medicine, Miami, FL

Abstract

Purpose—Conjunctival microvascular responses may be a surrogate metric of efferent neural pathway function innervating the ocular surface as changes in blood flow occur within seconds after a stimulus. As somatosensory dysfunction may partially underlie dry eye (DE), in this study we evaluate whether bulbar conjunctival microvascular alterations correlate with various aspects of DE.

Methods—Fifty-six DE patients were prospectively recruited from a Veterans Affairs ophthalmology clinic over an 11-month period. DE symptoms and ocular pain were assessed along with DE signs. A novel functional slit lamp biomicroscope (FSLB) was used to image the temporal bulbar conjunctiva from the right eye before and after central corneal stimulation with an air puff. Blood flow velocities were measured and noninvasive microvascular perfusion maps (nMPMs) were created.

Results—The bulbar blood flow velocity was 0.50 ± 0.15 mm/s at baseline and increased to 0.55 ± 0.17 mm/s after stimulation ($P < 0.001$); the average change in velocity was 0.05 ± 0.09 . nMPMs values and venule diameter, on the other hand, did not significantly increase after stimulation (1.64 ± 0.004 at baseline, 1.65 ± 0.04 after stimulation, $P = 0.22$ and 22.13 ± 1.84 μ m at baseline, 22.21 ± 2.04 μ m after stimulation, $P = 0.73$, respectively). Baseline blood flow velocity positively associated with Schirmer scores ($r = 0.40$, $P = 0.002$). Those with higher self-rated wind hyperalgesia demonstrated less change in blood flow velocity ($r = -0.268$, $P = 0.046$) after air stimulation on the central cornea.

Corresponding author: Anat Galor, MD, MSPH, Department of Ophthalmology, Miami Veteran Affairs Medical Center 1201 NW 16th Street, Miami, FL 33125, USA. Tel: 305-326-6000. Fax: 305-575-3312.; AGalor@med.miami.edu.

Publisher's Disclaimer: This is a PDF file of an unedited manuscript that has been accepted for publication. As a service to our customers we are providing this early version of the manuscript. The manuscript will undergo copyediting, typesetting, and review of the resulting proof before it is published in its final citable form. Please note that during the production process errors may be discovered which could affect the content, and all legal disclaimers that apply to the journal pertain.

Conflict of Interest: No conflicting relationship exists for any author.

Conclusion—Conjunctival blood flow velocity, but not vessel diameter or complexity, increases after wind stimuli. Baseline flow positively correlated with Schirmer scores while change in flow negatively correlated with self-reported wind hyperalgesia.

Keywords

Blood flow velocity; corneal sensitivity; fractal dimension; neuropathic ocular pain; functional slit lamp biomicroscopy

I. Introduction

Dry eye (DE) is a heterogeneous disease of the ocular surface, including but not limited to the lacrimal functional unit (LFU),¹ that affects millions of men and women in the United States.² It is characterized by symptoms of various intensity that may include ocular pain (described as dryness, burning, and aching) and visual complaints (fluctuating, blurry vision), both of which can reduce quality of life.³ Ocular surface findings are variable in DE and may include alterations in the quantity and quality of tears, ocular surface irregularity, and inflammation. To further complicate matters, it is well established that the symptoms and signs of DE do not correlate with each other.^{4, 5} In a prospective study of 263 male veterans, less than 10% of the variability in symptoms was explained by measured tear film parameters.⁵ This suggests that factors beyond ocular surface status are important in causing symptoms in certain individuals. It is not surprising, therefore, that some patients have persistent symptoms while on DE therapies targeting the ocular surface.⁶

A potential cause of ocular pain complaints in some DE patients may be neuropathic ocular pain (NOP), which occurs when there is damage and subsequent dysfunction in the corneal somatosensory system.⁷ There is a growing understanding that many patients diagnosed with DE describe features of neuropathic pain, including characterizing their ocular pain as “hot burning” and reporting evoked pain to wind and light.⁸ The superficial location and rich density of the corneal primary afferents, integrated between superficial epithelial cells, makes them vulnerable to repeated injury in the setting of ocular surface stress, minor trauma, or disease. Episodic or ongoing damage to the free corneal nerve endings through tear evaporation, temperature drop, and hyperosmolarity may result in nerve injury, altered neuronal healing, maladaptive neuroplasticity, and prolonged hypersensitivity to normally non-noxious stimuli both in peripheral and central nerves in the corneal somatosensory pathway.⁷

Several groups have used the Belmonte esthesiometer to study the afferent component of the corneal somatosensory pathway in DE patients.^{9–12} Interestingly, some studies found reduced corneal sensitivity to mechanical, chemical, and thermal stimuli compared to controls,^{10, 12} while others found increased sensitivity to mechanical stimuli.¹¹ Few studies, however, have focused on efferent neural pathways innervating the ocular surface, beyond studying tear production and blink rate.^{13, 14}

Efferent neural pathways to the ocular surface include autonomic fibers to the lacrimal glands, conjunctiva, meibomian glands, conjunctival blood vessels, and sensory nerves. Both parasympathetic and sympathetic nerves may be important in the context of ocular surface

pain because they can affect tear production, local blood flow, and sensory neuronal function (excitability and sensitivity to stimuli).¹⁵ Yet, study of the efferent innervation of the ocular surface is mainly limited by a lack of a technology with which to measure such efferent responses.

In this study, we evaluate a new technology, termed “functional slit lamp biomicroscopy (FSLB),” in which a Nikon slit lamp is modified by addition of a Canon digital camera to improve the magnification (~150×). In a previous study, we demonstrated that this imaging system quantitatively measured microvascular network density and hemodynamics.^{16, 17} Furthermore, this instrument was used to measure capillary blood flow before and after contact lens wear.¹⁶ The finding of an immediate increase in conjunctival blood flow suggested a neurally mediated response. In this study, we applied our new technology to study vascular responses in patients with a variety of DE and ocular pain complaints to test our hypothesis that patients with NOP symptoms have alterations in their conjunctival microcirculation responses compared to patients without such complaints.

II. Methods

A. Study Population

Patients with otherwise healthy eyelid and corneal anatomy were prospectively recruited from the Miami Veterans Affairs (VA) Healthcare System eye clinic between October 2014 and May 2015 and underwent a complete ocular surface examination. Patients were excluded from participation if they wore contact lenses, underwent refractive surgery, used ocular medications with the exception of artificial tears, had ocular comorbidities (pterygium, glaucoma, infection), had HIV, sarcoidosis, graft-versus-host disease or a collagen vascular disease, or had had cataract surgery within the last 6 months or any glaucoma or retinal surgery. Informed consent was obtained from all patients. Approval of the Miami VA Institution Review Board was obtained to allow the prospective evaluation of patients. The study was conducted in accordance with the principles of the Declaration of Helsinki and complied with the requirements of the United States Health Insurance Portability and Accountability Act.

B. Data Collected

1. Demographics and Comorbidities—Information on demographics, concomitant medical conditions, and medications were obtained, with a focus on conditions and medications that can affect blood vessel caliber and velocity.

2. Dry Eye Symptoms and Ocular Pain Complaints—For each individual, demographic information, past ocular and medical history, and medication information was collected. Patients filled out standardized questionnaires regarding DE symptoms, including the dry eye questionnaire 5 (DEQ5)¹⁸ and ocular surface disease index (OSDI [score 0–100]).¹⁹ Standard pain questionnaires were used to assess for the presence and quality of ocular pain. A numerical rating scale (NRS) for ocular pain intensity (score 0–10) was used to assess the “average intensity of eye pain during the past week.” The Neuropathic Pain Symptom Inventory (NPSI [score 0–100]) was used to quantify clinically relevant

dimensions of neuropathic pain.²⁰ For the evoked pain subsection of the NPSI, we replaced the three original questions regarding the severity of allodynia or hyperalgesia caused by 1) light touch, 2) pressure, or 3) contact with something cold on the skin, with questions specific to ocular allodynia or hyperalgesia [eye pain caused or increased by 1) wind, 2) light, and 3) heat or cold. Our strategy was to use both standardized assessments of dry eye (DEQ5 and OSDI) and standardized assessments of pain (NRS, NPSI) that we previously found could characterize ocular complaints²¹ and predicted a more severe and persistent dry eye course.^{8, 22} In this way, our research can be translated to other populations in which these standard dry eye metrics are used, but also specifically assesses subjective metrics that we believe are important in evaluating corneal somatosensory function.²³ In fact, the 0–10 NRS has been validated as a measure of pain intensity across multiple populations^{24–28} and has been recommended for use as the primary outcome metric in clinical trials for chronic pain.²⁹ We found that items on the NPSI-Eye (wind hyperalgesia, light allodynia) correlated well with similar questions on the OSDI (“Have your eyes felt uncomfortable in windy conditions?” “Eyes that are sensitive to light?”). Correlations were $r=0.687$, $p<0.0005$ and $r=0.70$, $p<0.0005$, respectively.

3. Belmonte Esthesiometry—The tip of the esthesiometer (0.5 mm in diameter) was placed perpendicular to, and 4 mm from, the surface of the cornea of the right eye. Stimulation consisted of pulses of air at room temperature (approximately 23 to 26°C) applied to the corneal surface. The method of limits, using ascending series only, was used to measure thresholds. For detection threshold measurements, subjects were presented with a stimulus immediately following a blink and were asked to indicate by pressing a button whether they felt the stimulus. The initial flow rate was set at a level below threshold (50 mL/min for most individuals) and increased by 10 mL/min (with 15 second intervals between stimuli) until the subject stated that they felt the stimulus (detection threshold) or the maximum allowable flow rate (400 mL/min) was reached. To estimate pain threshold, the flow rate was further increased beyond the detection threshold in 10 mL/min increments until the subject reported the stimulus as painful, or the maximum allowable flow rate (400 mL/min) was reached. Detection and pain thresholds were defined as the average of two such trials.

4. Ocular Surface Evaluation—All patients underwent tear film assessment, including the following measurements:

1. Tear osmolality (Tear LAB, San Diego, CA) once in each eye;
2. Ocular surface inflammation (Inflammadry, RPS, Tampa, FL);
3. Tear evaporation measured via tear film breakup time (TFBUT). 5 μ l fluorescein was placed, 3 measurements taken in each eye and averaged;
4. Corneal epithelial cell disruption according to corneal staining (National Eye Institute [NEI] scale³⁰ Five areas of cornea were assessed, with score 0–3 in each, total score equaling 0–15);
5. Tear production measured via Schirmer strips with anesthesia; and

6. Meibomian gland assessment. Eyelid vascularity was graded on a scale of 0 to 3 (0=none; 1= mild; 2=moderate; 3=severe engorgement) and meibum quality on a scale of 0 to 4 (0=clear; 1=cloudy; 2=granular; 3=toothpaste; 4=no meibum extracted).

5. Functional Slit Lamp Imaging—The FSLB imaging system composed of a digital camera and a traditional slit lamp was used in our study. As described in our previous study,¹⁷ the camera has a Movie Crop Function (MCF) that uses a center portion of pixels on the camera chip to generate an equivalent of $\sim 7\times$ magnification for high-speed video recording at 60 frames per second (fps) without the loss of image quality. With the built-in optical magnifications of up to $25\times$ in the slit lamp, the total magnification can be set up to $\sim 175\times$. We demonstrated in our previous study that this imaging system is capable of capturing the movement of red blood cells (RBC)/RBC clusters, which allows the blood flow velocity and vessel diameter to be measured.^{16, 17} In the present study, MCF with the magnification of $175\times$, a field of view of $1.22 \times 0.91 \text{ mm}^2$, and an image size of 640×480 pixels (pixel interval: $1.905 \mu\text{m}$) was utilized. Six different locations of the temporal bulbar conjunctiva were imaged, which were $\sim 1 \text{ mm}$ away from the limbus, covering a total area of $\sim 6 \times 4 \text{ mm}^2$ (Figure 1). In a previous publication, we reported how many blood vessels were needed to represent venule velocity and diameter in the entire bulbar conjunctiva.¹⁷ We used varying numbers of venules per subject in five subjects to determine that a sample size of 15 produced an acceptable standard error of 15%. Based on this, in the current study we imaged six different locations on the temporal bulbar conjunctiva, which assured that more than 15 blood vessels were recorded and analyzed per subject.

Custom software was used for the quantification of microvascular morphology and hemodynamics, as described in our previous studies.^{16, 17} The software was used to semi-automatically process the video clips to yield vessel diameters, lengths, vessel covering areas, and velocities for all measureable venules. In this study, only conjunctival venules were analyzed for blood flow velocity because the conjunctival pre-capillary arteriole blood flow velocity can be impacted by the pulse.³¹ Venules were distinguished from arterioles based on their diameter (bulbar conjunctiva arterioles are smaller than venules) and by the direction of flow (venule collected flow from branches in the bifurcation). The average diameter of vessels was calculated based on images converted from the video clips in which the velocity was measured. The vessel walls were outlined and marked in green and blue lines as shown in Figure 2B. The diameter of venules was found to differ by person with a range from 9 to $30 \mu\text{m}$. In a previous study, we demonstrated that a sample size of 15 vessels produced an acceptable standard error of 15%.¹⁷ While we did not image the same vessels before and after air stimulation, we averaged over 30 selected vessels from each eye and averaged them to represent the blood flow velocity of the temporal bulbar conjunctiva.

The measurement of blood flow velocity was based on the space-time image technique.^{16,32} For each field, at least half a second of video clip was collected and converted to at least 30 continuous frames. The first frame of the video clip was used for registering all frames to compensate for eye motion using custom software. In the spatial temporal image, we marked at least three slopes of multiple bands, determined by marking the starting and terminal points) (Figure 2). Then, the average axial blood flow velocity was calculated automatically

from these slopes. The accuracy and repeatability of this method has been reported in one of our previous study.³³

For the microvascular network calculations, we developed a single shot method to generate the nMPMs. We used a built-in green filter and $16 \times$ magnifications to obtain a field of view of about $15.70 \times 10.47 \text{ mm}^2$. A diffuse filter was then used to take the $3,456 \times 2,304$ pixel image of the temporal bulbar conjunctiva.¹⁶ We processed the segmented nMPMs using monofractal analyses (D_{box}) as described in detail in Figure 3.

C. Statistical Analysis

Data were entered into a standardized database. Statistical analyses were performed using SPSS 22.0 (SPSS Inc, Chicago, IL) statistical package. Descriptive statistics were used to summarize patient demographic and clinical information. Paired t test methodology was used to compare parameters before and after air stimulation. Correlations (Pearson and Spearman) were used to evaluate the strength of association between functional slit lamp imaging parameters and severity of DE symptoms and signs. Student t-tests and Mann-Whitney U tests were used (as appropriate) to evaluate for differences in means (or medians) between groups. P-values <0.05 were considered significant.

III. Results

A. Study Population

The mean age of the population was 61 years, with a standard deviation (SD) of 10 (Table 1); 85% (n=34) of the patients were male, 45% (n=25) self-characterized themselves as white, and 21% (n=12) as Hispanic. Our population had a range of DE symptoms and signs (Table 1) and, similar to prior publications, there were no correlations between subjective and objective DE parameters. With regard to symptoms, 7 patients (12.5%) had no dry eye symptoms (DEQ5 $<$ 6), 16 (28.6%) had mild-moderate symptoms (DEQ5 6–11), and 33 (58.9%) had severe symptoms (DEQ5 \geq 12).

B. Blood Flow Velocity and Fractal Dimension before and after Air Stimuli

Fifty-six cases of blood flow velocities and 42 cases of nMPMs were analyzed. Fourteen cases of nMPMs images were excluded due to insufficient image quality (due to blinking). The bulbar blood flow velocity was $0.50 \pm 0.15 \text{ mm/s}$ at baseline and increased significantly to $0.55 \pm 0.17 \text{ mm/s}$ after air stimuli, representing on average a 10% ($0.55 - 0.50 / 0.50$) increase in blood flow ($P < 0.001$, Figure 4A). The average change in velocity was 0.05 ± 0.09 . However, as the lowest blood flow observed in our patients was 0.24 mm/s (and not 0), we re-examined the percent increase when setting the lower limit of flow to 0.24. In this manner, the average percent increase after air stimulation was 19.2%, calculated as follows:

$$\frac{([\text{post-stimulation blood flow mean (0.55)} - \text{lowest blood flow velocity observed (0.24)}] - [\text{pre-stimulation blood flow mean (0.50)} - \text{lowest blood flow velocity observed (0.24)}])}{[\text{pre-stimulation blood flow mean (0.50)} - \text{lowest blood flow velocity observed (0.24)}]}$$

Our baseline value of 0.50 mm/s falls slightly under the range of blood flow velocities previously reported in venules and arterioles (range, 0.52 to 3.26 mm/s).^{16, 31, 32, 34}

Bulbar conjunctival vessel density, on the other hand, was not significantly different between baseline (1.64 ± 0.04) and after stimulation (1.65 ± 0.04 , $P=0.22$, Figure 4B). Average vessel diameter was likewise similar before ($22.13 \pm 1.84 \mu\text{m}$) and after air stimulation ($22.21 \pm 2.04 \mu\text{m}$, $P=0.724$, Figure 4C).

C. Correlations between Baseline Conjunctival Microvascular Parameters and Responses and Demographics and Comorbidities

None of the demographic characteristics, comorbidities, or medications studied significantly impacted conjunctival microvascular findings except that patients with benign prostatic hypertrophy (BPH) had less of a change in velocity compared to those without BPH (-0.01 ± 0.07 mm/s versus 0.07 ± 0.08 mm/s, $P=0.003$).

D. Correlations between Baseline Functional Slit Lamp Parameters and DE Symptoms and Signs

Baseline blood flow velocity positively correlated with Schirmer scores ($r=0.404$, $P=0.002$) and negatively with eyelid vascularity ($r=-0.274$, $P=0.043$ [Table 2]). Baseline network complexity negatively correlated with baseline pain symptoms (NRS $r=-0.319$, $P=0.04$ and light allodynia $r=-0.337$, $P=0.029$) and ocular surface signs (meibum quality -0.329 , $P=0.036$; eyelid vascularity -0.34 , $P=0.03$; pain thresholds $r=-0.322$, $P=0.04$). A smaller difference between pain and detection thresholds negatively correlated with both baseline velocity and network complexity.

E. Correlations between Change in Conjunctival Microvascular Blood Flow Velocity and DE Symptoms and Signs

Subjects with higher self-rated wind hyperalgesia demonstrated less change in blood flow velocity ($r=-0.268$, $P=0.046$ [Figure 5]) after air stimulation on the central cornea (Table 3). No other DE symptom, ocular pain complaint, objective ocular surface metric, ocular surface inflammation (via Inflammadry, RPS, Tampa FL) or corneal detection or pain thresholds significantly correlated with change in velocity. However, subjects with ocular surface inflammation did have higher velocities post-stimulation (0.65 ± 0.15 mm/s) compared to those without inflammation (0.52 ± 0.16 mm/s; $p=0.02$).

IV. Discussion

We found that after corneal stimulation with air stimuli, blood velocity through the bulbar venules significantly increased, while microvascular density and vessel diameter did not significantly differ. Our findings are similar to those from our previous work in which contact lens placement, rather than air, was used as a stimulus. In the previous study, we found an immediate increase in blood flow after contact lens placement, and after 6 hours of wear, an increase in both flow and microvascular network density.¹⁶ In a similar manner, Chueng et al reported that longterm (>2 years) contact lens wearers displayed microvascular changes in their conjunctival microcirculation.³⁵ The results of these studies imply that

changes in velocity are immediate as opposed to morphological changes in conjunctival vessels, which take longer to manifest. We hypothesize that efferent parasympathetic responses are responsible for the noted increased blood flow in both models.

Increased blood flow after stimulation has also been observed in other areas of the body.^{36–38} For example, transcorneal stimulation of trigeminal nerve endings caused an immediate and robust increase in blood flow in the cerebral arteries.³⁹ In a similar manner, capsaicin and saline applied to the human forehead, with and without iontophoresis, led to an immediate increase in dermal blood flow.⁴⁰

Similar to network density, vessel diameter did not change after air puff stimuli. A possible explanation for this may be that we measured venules as opposed to arterioles in this study.¹⁶ Although venules have been confirmed to be important in microvascular pressure and flow regulation, their responses to stimuli (such as light, flow, and pressure) have been reported as minor compared to arterioles.^{16, 41} It is also interesting that no vessel alterations were seen in patients with diabetes compared to individuals without this comorbidity. This is in contradiction to previous reports in which the presence of diabetes associated with significantly increased venule diameter.^{42, 43} Potential explanations for the discrepancy include our unique patient population (which included a limited number of patients with diabetes and the presence of confounding ocular comorbidities), differences in statistical analysis (qualitative^{42, 43} vs quantitative), and different imaging strategies.

Studying microvascular responses in the conjunctiva may provide insight on the corneal somatosensory pathway that is now increasingly understood to be involved in various manifestations of DE. The pathway originates from free nerve endings interdigitating between corneal epithelial cells. The cell bodies of these nerves sit in the trigeminal ganglion, and their proximal projections synapse in the trigeminal subnucleus interpolaris/subnucleus caudalis (Vi/Vc) transition zone and in the subnucleus caudalis/upper cervical transition zone (Vc/C₁₋₂). Second-order neurons decussate and join the contralateral spinothalamic pathways and synapse in the thalamus. Third-order neurons then relay information to the supra-spinal centers, including the somatosensory cortex.⁷ This ascending pathway is linked to efferent pathways, which have multiple innervations, including to the lacrimal gland (e.g., tear production), eyelid (e.g., blinking) and conjunctival blood vessels (e.g., blood flow). Previous studies have attempted to elucidate these efferent pathways, mostly by measuring tear secretion evoked by mechanical and chemical stimuli on the cornea, with central corneal mechanical stimulation evoking the strongest lacrimation reflex.^{13, 14} Yet, other pathways of efferent output to the ocular surface, beyond tear secretion, remain relatively underinvestigated.

In this study, we assessed microvascular responses after trigeminal stimulation in patients with DE as a potential endpoint to study efferent pathways. With respect to velocity, we found that patients with reduced levels of tear production had slower blood flow at baseline. This finding may imply that in such patients, there is an imbalance of autonomic mechanisms towards a predominance of sympathetically mediated mechanisms (versus parasympathetic). Increased sympathetic activity has been reported after nerve and tissue

injuries⁴⁴, and this may mediate pain states involving the trigeminal system in select patients.⁴⁵

Although interspecies differences exist, sympathetic efferents have been identified in the cornea.^{15, 46} These corneal sympathetic efferents project from the ipsilateral superior cervical ganglion and are thought to influence physiologic processes in the cornea, such as ion transport and hydration, mitogenesis and wound healing, and neuronal sensitivity.¹⁵ Not yet explored, however, is their potential role in the pathophysiology of DE. Sympathetic overactivity via increased sympathetic efferent–somatosensory neuronal coupling may result in peripheral neuronal sensitization and enhanced pain responses after peripheral nerve injury, and as such may be involved in sensitization of peripheral afferents in the cornea. This might be the case in our patient subpopulation with reduced levels of tear production.

On the other hand, we found that patients with self-reported wind hyperalgesia had a dampened response to air simulation, with less of a flow increase compared to those without this complaint. While the effect magnitude of the effect was not large (the degree of blood flow increase explained ~7% of variability in subjective wind hyperalgesia), this value is in line with other studies that evaluated the relationship between somatosensory function and DE symptoms.⁴⁷

In our previous study, we found a similar magnitude in the relationship between self-reported wind hyperalgesia and detection ($r=-0.25$) and pain ($r=-0.23$) corneal thresholds.²³ It is interesting that wind hyperalgesia significantly correlated with microvascular responses, as we previously found that this complaint correlated with DE symptom severity and persistence,⁸ a decreased response to artificial tears,²² and increased corneal sensitivity to an air puff.²³ Taken together, these findings provide criterion validity (how well a question obtains the same results as other approaches measuring the same characteristic⁴⁸) for the importance of wind hyperalgesia as a sign of corneal somatosensory dysfunction.

These findings may imply that contrary to findings described above, in patients with wind hyperalgesia, there is an imbalance of autonomic mechanisms towards a predominance of parasympathetically-mediated mechanisms. Raised parasympathetic hyperactivity via the sphenopalatine ganglion has been described in other facial pain conditions, such as cluster headache.^{49,50} If parasympathetic efferents are basally activated, blood vessels may have reached maximal dilatation, explaining the blunted blood flow response after air stimulation in this subpopulation. These findings suggest dichotomous DE patient populations. In addition, significant associations were noted between DE symptoms and signs and baseline vessel complexity, with higher DE symptoms and more abnormal signs associating with less complexity. The pathophysiological explanations for the noted observations are not clear.

While the results of this preliminary study are interesting, we recognize that they need to be considered bearing in mind the study limitations. First, our study was conducted at a Veterans Affairs Hospital, and therefore our population consists of predominantly older males, most of whom had either symptoms or one or more signs of DE. Second, our cross-sectional study design precludes commenting on persistence or change in DE symptoms, signs, and functional slit lamp parameters over time. Third, we did not image the blood flow

and diameter of bulbar arterioles in this study due to technology limitations. Fourth, our numbers are small, limiting our power to detect statistically significant differences in parameters. Despite these limitations, this study is the first to study bulbar conjunctiva microvascular changes in response to air stimuli in the context of DE.

V. Conclusion

Mechanical stimuli on the central cornea affect bulbar conjunctiva blood flow velocity overall and differentially in patients with NOP complaints. Our data provide support that DE patients are a heterogeneous group with differences in the function of their corneal somatosensory pathway, efferent responses to sensory stimuli, and autonomic status. Further studies, capturing both arteriole and venule flow, are needed to assess whether bulbar conjunctiva microvascular parameters can aid in the diagnosis of DE sub-types, guide treatment, and follow treatment response.

Acknowledgments

Financial Support: The funding organization had no role in the design or conduct of this research. The financial and material support of this paper comes from the Veterans Health Administration, Office of Research and Development, Clinical Sciences Research EPID-006-15S (Dr. Galor), R01EY026174 (Dr. Galor), NIH Center Core Grant P30EY014801, Research to Prevent Blindness Unrestricted Grant., UM SAC 2015-27R1 (JW), NIH Center Core Grant P30EY014801, NIH NIDCR RO1 DE022903 (Dr. Levitt), and the Department of Anesthesiology, Perioperative Medicine, and Pain Management, University of Miami Miller School of Medicine, Miami, FL. The University of Miami and Dr. Wang holds a pending patent for the technique used in the study and have the potential for financial benefits from its future commercialization. None of the other authors have any proprietary interest in any materials or methods.

References

1. Stern ME, Gao J, Siemasko KF, Beuerman RW, Pflugfelder SC. The role of the lacrimal functional unit in the pathophysiology of dry eye. *Exp Eye Res.* 2004; 78:409–16. [PubMed: 15106920]
2. The epidemiology of dry eye disease: report of the Epidemiology Subcommittee of the International Dry Eye WorkShop (2007). *Ocul Surf.* 2007; 5:93–107. No authors listed. [PubMed: 17508117]
3. Pouyeh B, Viteri E, Feuer W, Lee DJ, Florez H, Fabian JA, et al. Impact of ocular surface symptoms on quality of life in a United States veterans affairs population. *Am J Ophthalmol.* 2012; 153:1061–66 e3. [PubMed: 22330309]
4. Schein OD, Tielsch JM, Munoz B, Bandeen-Roche K, West S. Relation between signs and symptoms of dry eye in the elderly. A population-based perspective. *Ophthalmology.* 1997; 104:1395–401. [PubMed: 9307632]
5. Galor A, Feuer W, Lee DJ, Florez H, Venincasa VD, Perez VL. Ocular surface parameters in older male veterans. *Invest Ophthalmol Vis Sci.* 2013; 54:1426–33. [PubMed: 23385801]
6. Stonecipher K, Perry HD, Gross RH, Kerney DL. The impact of topical cyclosporine A emulsion 0.05% on the outcomes of patients with keratoconjunctivitis sicca. *Curr Med Res Opin.* 2005; 21:1057–63. [PubMed: 16004673]
7. Galor A, Levitt RC, Felix ER, Martin ER, Sarantopoulos CD. Neuropathic ocular pain: an important yet undervalued feature of dry eye. *Eye (Lond).* 2015; 29:301–12. [PubMed: 25376119]
8. Galor A, Zlotcavitch L, Walter SD, Felix ER, Feuer W, Martin ER, et al. Dry eye symptom severity and persistence are associated with symptoms of neuropathic pain. *Br J Ophthalmol.* 2015; 99:665–8. [PubMed: 25336572]
9. Benitez-Del-Castillo JM, Acosta MC, Wassfi MA, Diaz-Valle D, Gegundez JA, Fernandez C, et al. Relation between corneal innervation with confocal microscopy and corneal sensitivity with noncontact esthesiometry in patients with dry eye. *Invest Ophthalmol Vis Sci.* 2007; 48:173–81. [PubMed: 17197530]

10. Bourcier T, Acosta MC, Borderie V, Borrás F, Gallar J, Bury T, et al. Decreased corneal sensitivity in patients with dry eye. *Invest Ophthalmol Vis Sci.* 2005; 46:2341–5. [PubMed: 15980220]
11. De Paiva CS, Pflugfelder SC. Corneal epitheliopathy of dry eye induces hyperesthesia to mechanical air jet stimulation. *Am J Ophthalmol.* 2004; 137:109–15. [PubMed: 14700652]
12. Gallar J, Morales C, Freire V, Acosta MC, Belmonte C, Duran JA. Decreased corneal sensitivity and tear production in fibromyalgia. *Invest Ophthalmol Vis Sci.* 2009; 50:4129–34. [PubMed: 19324850]
13. Acosta MC, Peral A, Luna C, Pintor J, Belmonte C, Gallar J. Tear secretion induced by selective stimulation of corneal and conjunctival sensory nerve fibers. *Invest Ophthalmol Vis Sci.* 2004; 45:2333–6. [PubMed: 15223813]
14. Situ P, Simpson TL. Interaction of corneal nociceptive stimulation and lacrimal secretion. *Invest Ophthalmol Vis Sci.* 2010; 51:5640–5. [PubMed: 20554608]
15. Marfurt CF. Sympathetic innervation of the rat cornea as demonstrated by the retrograde and anterograde transport of horseradish peroxidase-wheat germ agglutinin. *J Comp Neurol.* 1988; 268:147–60. [PubMed: 3360982]
16. Jiang H, Zhong J, DeBuc DC, Tao A, Xu Z, Lam BL, et al. Functional slit lamp biomicroscopy for imaging bulbar conjunctival microvasculature in contact lens wearers. *Microvasc Res.* 2014; 92:62–71. [PubMed: 24444784]
17. Wang L, Yuan J, Jiang H, Yan W, Cintron-Colon HR, Perez VL, et al. Vessel sampling and blood flow velocity distribution with vessel diameter for characterizing the human bulbar conjunctival microvasculature. *Eye Contact Lens.* 2016; 42(2):135–40. DOI: 10.1097/ICL.000000000000146 [PubMed: 25839347]
18. Chalmers RL, Begley CG, Caffery B. Validation of the 5-Item Dry Eye Questionnaire (DEQ-5): Discrimination across self-assessed severity and aqueous tear deficient dry eye diagnoses. *Cont Lens Anterior Eye.* 2010; 33:55–60. [PubMed: 20093066]
19. Schiffman RM, Christianson MD, Jacobsen G, Hirsch JD, Reis BL. Reliability and validity of the Ocular Surface Disease Index. *Arch Ophthalmol.* 2000; 118:615–21. [PubMed: 10815152]
20. Bouhassira D, Attal N, Fermanian J, Alchaar H, Gautron M, Masquelier E, et al. Development and validation of the Neuropathic Pain Symptom Inventory. *Pain.* 2004; 108:248–57. [PubMed: 15030944]
21. Kalangara JP, Galor A, Levitt RC, Covington DB, McManus KT, Sarantopoulos CD, et al. Characteristics of ocular pain complaints in patients with idiopathic dry eye symptoms. *Eye Contact Lens.* 2016 AU: Please provide complete information.
22. Galor A, Batawi H, Felix ER, Margolis TP, Sarantopoulos KD, Martin ER, et al. Incomplete response to artificial tears is associated with features of neuropathic ocular pain. *Br J Ophthalmol.* 2016; 100:745–9. [PubMed: 26377416]
23. Spierer O, Felix ER, McClellan AL, Parel JM, Gonzalez A, Feuer WJ, et al. Corneal mechanical thresholds negatively associate with dry eye and ocular pain symptoms. *Invest Ophthalmol Vis Sci.* 2016; 57:617–25. [PubMed: 26886896]
24. Caraceni A, Cherny N, Fainsinger R, Kaasa S, Poulain P, Radbruch L, et al. Pain measurement tools and methods in clinical research in palliative care: recommendations of an Expert Working Group of the European Association of Palliative Care. *J Pain Symptom Manage.* 2002; 23:239–55. [PubMed: 11888722]
25. Farrar JT, Young JP Jr, LaMoreaux L, Werth JL, Poole RM. Clinical importance of changes in chronic pain intensity measured on an 11-point numerical pain rating scale. *Pain.* 2001; 94:149–58. [PubMed: 11690728]
26. Paice JA, Cohen FL. Validity of a verbally administered numeric rating scale to measure cancer pain intensity. *Cancer Nurs.* 1997; 20:88–93. [PubMed: 9145556]
27. Ferreira-Valente MA, Pais-Ribeiro JL, Jensen MP. Validity of four pain intensity rating scales. *Pain.* 2011; 152:2399–404. [PubMed: 21856077]
28. Jensen MP, Turner JA, Romano JM. What is the maximum number of levels needed in pain intensity measurement? *Pain.* 1994; 58:387–92. [PubMed: 7838588]

29. Dworkin RH, Turk DC, Farrar JT, Haythornthwaite JA, Jensen MP, Katz NP, et al. Core outcome measures for chronic pain clinical trials: IMMPACT recommendations. *Pain*. 2005; 113:9–19. [PubMed: 15621359]
30. Lemp MA. Report of the National Eye Institute/Industry workshop on Clinical Trials in Dry Eyes. *CLAO J*. 1995; 21:221–32. [PubMed: 8565190]
31. Koutsiaris AG, Tachmitzi SV, Papavasileiou P, Batis N, Kotoula MG, Giannoukas AD, et al. Blood velocity pulse quantification in the human conjunctival pre-capillary arterioles. *Microvasc Res*. 2010; 80:202–8. [PubMed: 20478318]
32. Shahidi M, Wanek J, Gaynes B, Wu T. Quantitative assessment of conjunctival microvascular circulation of the human eye. *Microvasc Res*. 2010; 79:109–13. [PubMed: 20053367]
33. Xu Z, Jiang H, Tao A, Wu S, Yan W, Yuan J, et al. Measurement variability of the bulbar conjunctival microvasculature in healthy subjects using functional slit lamp biomicroscopy (FSLB). *Microvasc Res*. 2015; 101:15–9. [PubMed: 26092682]
34. Cheung AT, Perez RV, Chen PC. Improvements in diabetic microangiopathy after successful simultaneous pancreas-kidney transplantation: a computer-assisted intravital microscopy study on the conjunctival microcirculation. *Transplantation*. 1999; 68:927–32. [PubMed: 10532529]
35. Cheung AT, Hu BS, Wong SA, Chow J, Chan MS, To WJ, et al. Microvascular abnormalities in the bulbar conjunctiva of contact lens users. *Clin Hemorheol Microcirc*. 2012; 51:77–86. [PubMed: 22240372]
36. Salar G, Ori C, Iob I, Costella GB, Battaglia C, Peserico L. Cerebral blood flow changes induced by electrical stimulation of the Gasserian ganglion after experimentally induced subarachnoid haemorrhage in pigs. *Acta Neurochir (Wien)*. 1992; 119:115–20. [PubMed: 1481737]
37. Suzuki N, Hardebo JE, Kahrstrom J, Owman C. Effect on cortical blood flow of electrical stimulation of trigeminal cerebrovascular nerve fibres in the rat. *Acta Physiol Scand*. 1990; 138:307–16. [PubMed: 2327261]
38. Morita-Tsuzuki Y, Hardebo JE, Bouskela E. Interaction between cerebrovascular sympathetic, parasympathetic and sensory nerves in blood flow regulation. *J Vasc Res*. 1993; 30:263–71. [PubMed: 8399987]
39. Atalay B, Bolay H, Dalkara T, Soylemezoglu F, Oge K, Ozcan OE. Transcorneal stimulation of trigeminal nerve afferents to increase cerebral blood flow in rats with cerebral vasospasm: a noninvasive method to activate the trigeminovascular reflex. *J Neurosurg*. 2002; 97:1179–83. [PubMed: 12450041]
40. Ibrahimi K, Vermeersch S, Danser A, Villalon C, van den Meiracker A, de Hoon J, et al. Development of an experimental model to study trigeminal nerve-mediated vasodilation on the human forehead. *Cephalalgia*. 2014; 34:514–22. [PubMed: 24391116]
41. Bishop JJ, Nance PR, Popel AS, Intaglietta M, Johnson PC. Diameter changes in skeletal muscle venules during arterial pressure reduction. *Am J Physiol Heart Circ Physiol*. 2000; 279:H47–57. [PubMed: 10899040]
42. Cheung AT, Ramanujam S, Greer DA, Kumagai LF, Aoki TT. Microvascular abnormalities in the bulbar conjunctiva of patients with type 2 diabetes mellitus. *Endocr Pract*. 2001; 7:358–63. [PubMed: 11585371]
43. Cheung AT, Tomic MM, Chen PC, Miguelino E, Li CS, Devaraj S. Correlation of microvascular abnormalities and endothelial dysfunction in Type-1 Diabetes Mellitus (T1DM): a real-time intravital microscopy study. *Clin Hemorheol Microcirc*. 2009; 42:285–95. [PubMed: 19628894]
44. Janig W, Levine JD, Michaelis M. Interactions of sympathetic and primary afferent neurons following nerve injury and tissue trauma. *Prog Brain Res*. 1996; 113:161–84. [PubMed: 9009734]
45. Janig W. Relationship between pain and autonomic phenomena in headache and other pain conditions. *Cephalalgia*. 2003; 23(Suppl 1):43–8.
46. Marfurt CF, Kingsley RE, Echtenkamp SE. Sensory and sympathetic innervation of the mammalian cornea. A retrograde tracing study. *Invest Ophthalmol Vis Sci*. 1989; 30:461–72. [PubMed: 2494126]
47. Situ P, Simpson TL, Fonn D, Jones LW. Conjunctival and corneal pneumatic sensitivity is associated with signs and symptoms of ocular dryness. *Invest Ophthalmol Vis Sci*. 2008; 49:2971–6. [PubMed: 18390645]

48. Spilker, B. Guide to clinical trials. New York: Raven Press; 1991. p. 315-6.
49. Drummond PD. Autonomic disturbances in cluster headache. Brain. 1988; 111(Pt 5):1199–209. [PubMed: 3179690]
50. Goadsby PJ. Pathophysiology of cluster headache: a trigeminal autonomic cephalgia. Lancet Neurol. 2002; 1:251–7. [PubMed: 12849458]

Author Manuscript

Author Manuscript

Author Manuscript

Author Manuscript

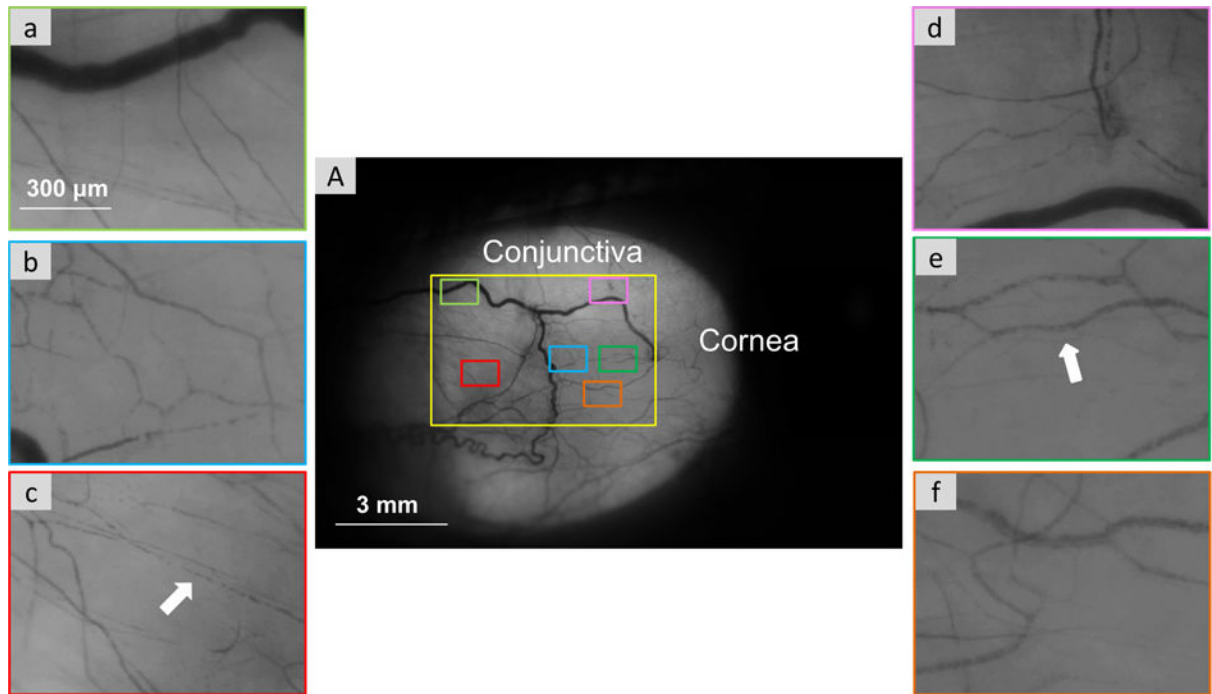


Figure 1. Temporal bulbar conjunctiva microvasculature imaged by the functional slit lamp biomicroscope. Videos clips were acquired from six locations which were homogeneously located on the temporal side of the bulbar conjunctiva (A). With $\times 175$ magnification, red blood cell clusters (white arrow) are shown in the six fields (a–f).

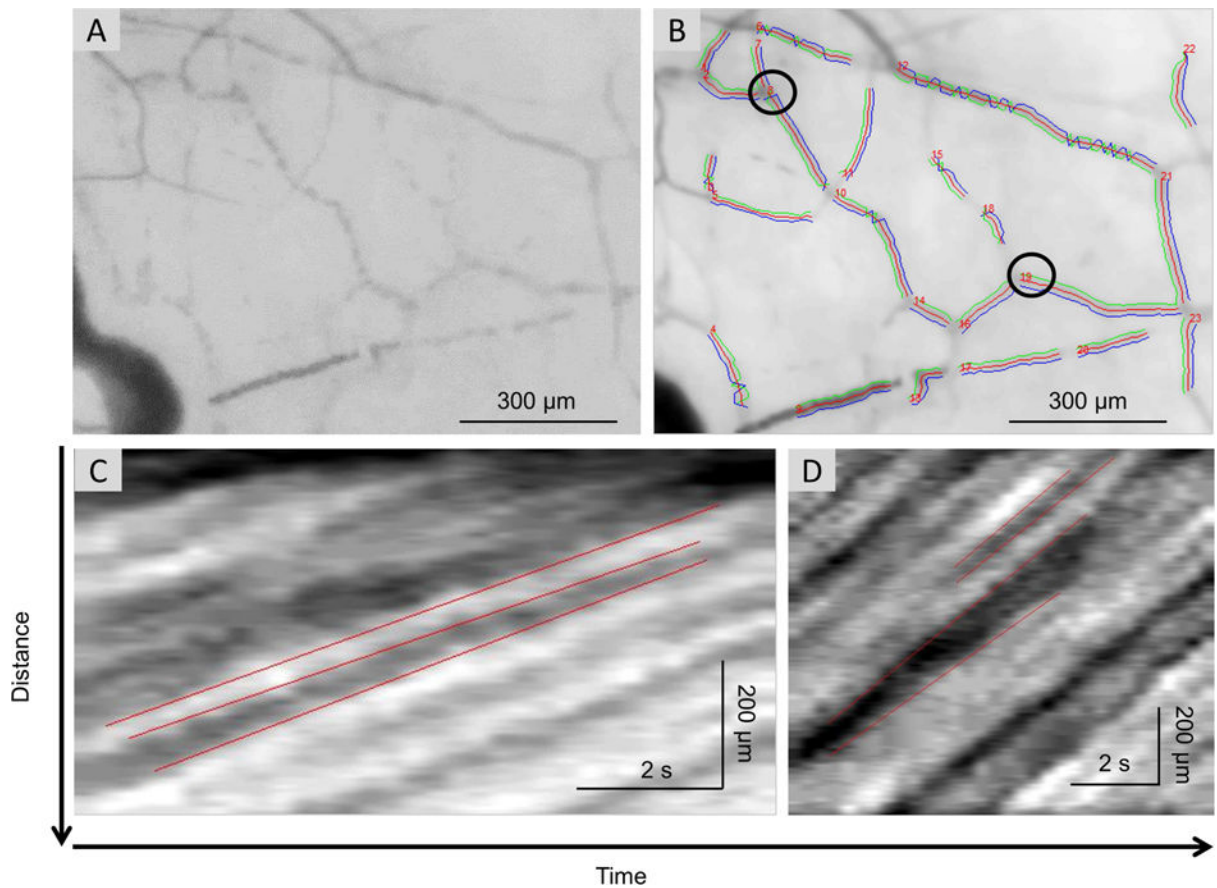


Figure 2.

Measurement of the vessel diameter and blood flow velocity. Custom software was developed and utilized to process the video clips obtained on the bulbar conjunctiva. The first frame (A) of the video clip was used for registering all frames to compensate for the eye motion. After that, all registered images were averaged and the blood vessels were segmented from the average image. The vessels were automatically identified and marked in numbers (B). The vessel walls were outlined and marked in green and blue lines for measuring the vessel diameter (B). By calculating the image intensity within the areas defined by the vessel walls, an intensity profile along the center line between these walls was generated for each frame. Using all intensity profiles of all frames in the video clips, a space-time image was obtained and used to measure the blood flow velocity. The slopes of the bands (i.e. moving distance over time) were manually outlined (marked in red lines) and calculated as the measurements of axial blood flow velocity (C for vessel No. 8, D for vessel No. 19).

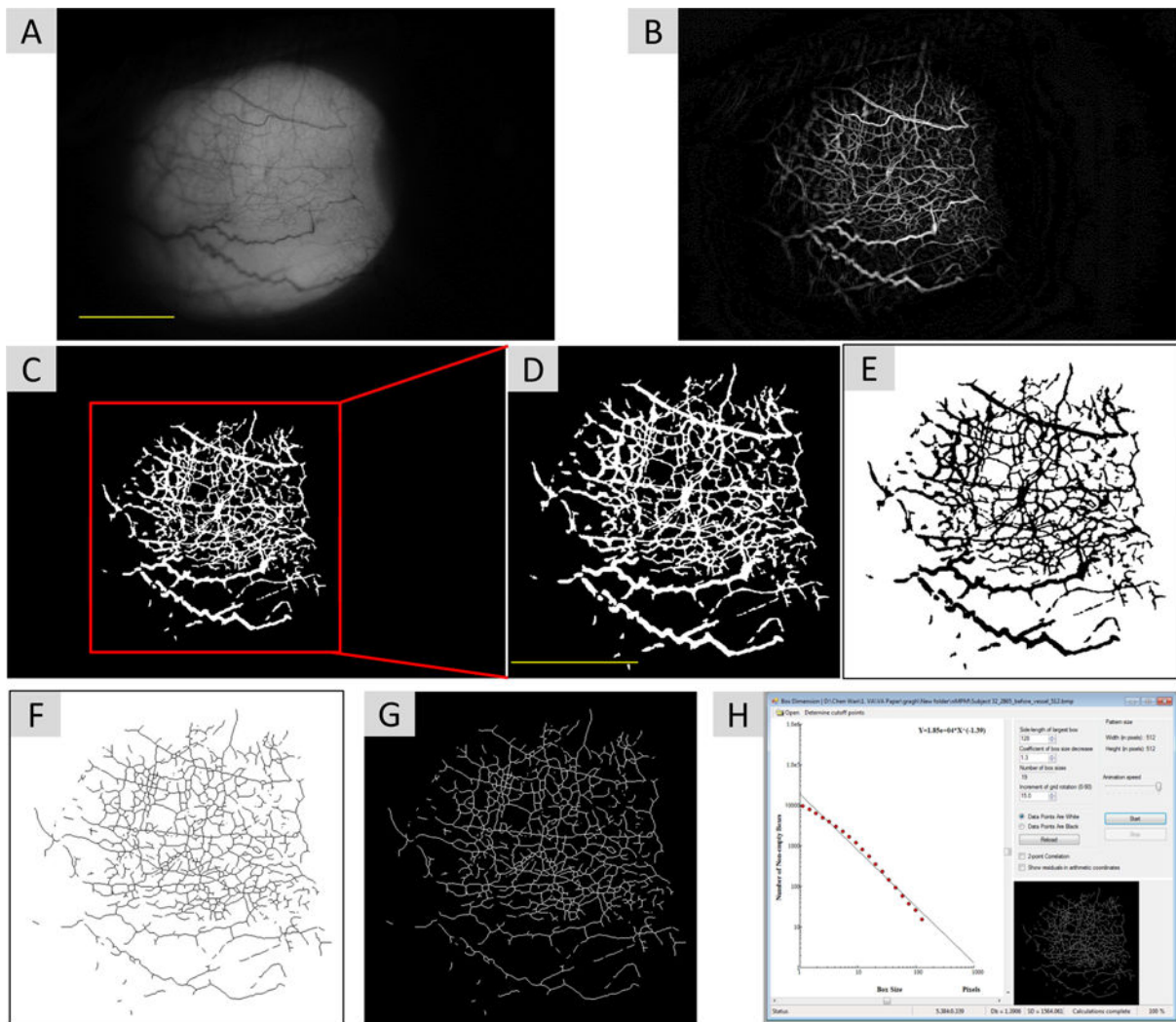


Figure 3.

Non-invasive microvascular perfusion maps (nMPMs) and fractal analysis. Custom software was developed to segment conjunctival vessels and to create the nMPMs for fractal analysis using a series of image processing procedures. The raw image was first resized from $3,456 \times 2,304$ pixels to $1,024 \times 683$ pixels (A). Imaging processing using morphological opening was performed to create nMPMs (B). Vessels were segmented (C) and the image was cropped a field of view 7.85×7.85 mm² containing 512×512 pixels (D). The cropped image was then inverted (E) and skeletonized (F). The image was further inverted back for fractal analysis (G) using monofractal analysis (i.e. box-counting, H). Bars=3 mm.

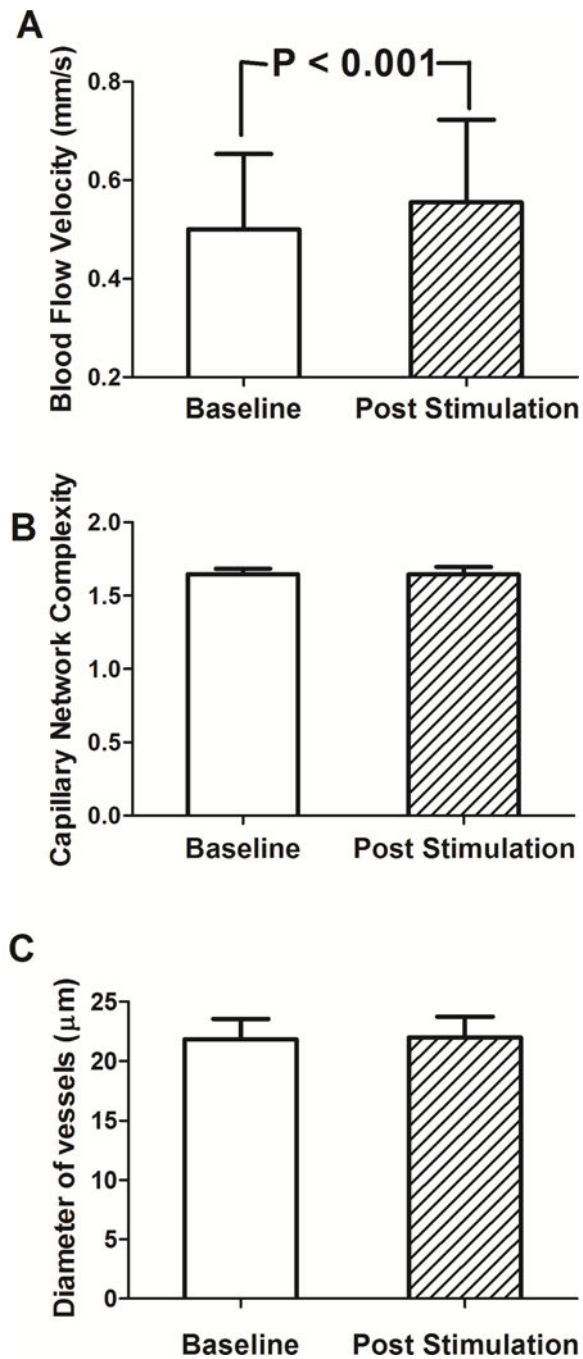


Figure 4. Bulbar conjunctival blood flow velocities, nMPMs, and vessel diameters were measured in DE patients before and after air stimulation. A. Blood flow velocity increased significantly after air stimuli ($P < 0.001$). B, C. Both fractal dimension and vessel diameter were not significantly different before and after air stimulation ($P = 0.22$, $P = 0.73$, respectively).

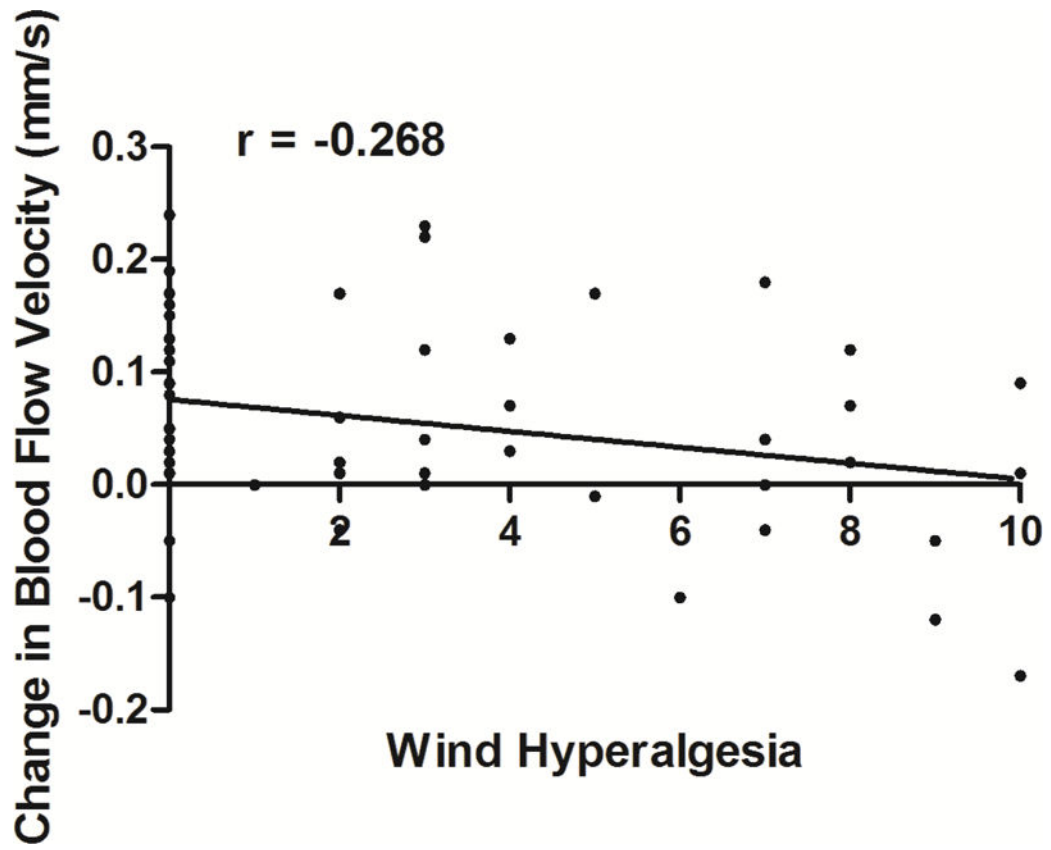


Figure 5. An inverse correlation is noted between change in conjunctival microvascular blood flow after mechanical stimulation and self-reported wind hyperalgesia ($r=-0.268$, $P=0.046$).

Table 1

Demographics and co-morbidities of the patient population (n=56)

Demographics	
Age, mean(SD)[range]	61(10) [34–87]
Race, white, n (%) black, n (%)	25 (44.6) 31 (55.4)
Gender, male, n (%)	49 (87.5)
Ethnicity, Hispanic, n (%)	12 (21.4)
Smoking, former, n (%) current, n (%)	20 (35.7) 26 (46.4)
Co-morbidities, n (%)	
Hypertension	41 (73.2)
Hypercholesterolemia	34 (60.7)
Diabetes	15 (26.8)
Arthritis	27 (48.2)
Sleep apnea	12 (21.4)
Benign prostatic hypertrophy	12 (21.4)
Medication use, n (%)	
Analgesics	34 (60.7)
Antidepressants	25 (44.6)
Anxiolytics	27 (48.2)
Antihistamine	7 (12.5)
Beta blocker	12 (21.4)
DE symptoms, mean(SD)[range]	
Dry eye questionnaire 5	11.4 (4.9) [0–20]
Ocular surface disease index	35.35 (23.09) [0–88.63]
Ocular pain, mean(SD)[range]	
NRS	3.39 (2.72) [0–9]
NPSI-Eye total	20.9 (22.2) [0–78]
Burning spontaneous pain	3.1 (3.3) [0–10]
Wind hyperalgesia	3.0 (3.4) [0–10]
Light allodynia	3.4 (3.4) [0–10]
Ocular signs[*], mean(SD)[range]	
Osmolarity, mOsm/L	304.9 (13.6) [287–360]
Tear break up time, seconds	12.1 (5.1) [4–30]
Corneal staining	1.1 (1.7) [0–6]
Schirmer's test, mm wetting at 5 minutes	15.9 (7.5) [3–32]
Meibum quality	1.7 (1.3) [0–4]
Eyelid vascularity	0.5 (0.7) [0–2]
Corneal sensitivity[*], mean(SD)[range]	

Demographics	
Detection thresholds, mL/min	89.7 (36.2) [20–160]
Pain thresholds, mL/min	232.0 (103.7) [50–410]
Functional slit lamp parameters[*], mean(SD)[range]	
Baseline velocity, mm/s	0.50 (0.15) [0.24–0.85]
Post air stimulus velocity, mm/s	0.55 (0.17) [0.26–0.96]
Network complexity	1.64 (0.04) [1.52–1.69]
Venule diameter, μm	22.13 (1.84) [17.13–27.13]

NRS=numerical rating scale, average ocular pain intensity, 1 week recall; NPSI-Eye=neuropathic pain symptom inventory modified for the eye; SD=standard deviation;

* values from right eye

Table 2

Correlations between baseline bulbar conjunctival microvasculature parameters and DE symptoms (including ocular pain) and signs

Continuous variables	Velocity Pearson r/Spearman rho	Network complexity Pearson r/Spearman rho	Vessel diameter Pearson r/Spearman rho
DE symptoms			
Dry eye questionnaire 5	0.001/0.059	-0.150/-0.114	0.074/0.134
Ocular surface disease index	0.088/0.081	-0.218/-0.238	0.133/0.116
Ocular pain			
NRS	0.084/-0.294	-0.319 */-0.294	0.167/0.147
NPSI-Eye total	0.045/0.012	-0.174/-0.249	0.066/0.070
Burning spontaneous pain	0.085/0.057	-0.137/-0.180	-0.031/-0.027
Wind hyperalgesia	-0.011/-0.013	-0.083/-0.094	0.045/0.033
Light allodynia	-0.030/-0.032	-0.337 */-0.290	0.250/0.250
Ocular signs			
Osmolarity [‡]	0.052/0.114	-0.023/0.004	-0.203/-0.209
Tear break up time [‡]	-0.025/-0.023	0.122/0.085	0.018/0.035
Corneal staining [‡]	0.137/0.162	0.184/0.249	0.064/0.026
Schirmer's test [‡]	0.404 */ 0.432 *	-0.101/-0.130	0.093/0.161
Meibum quality [‡]	-0.182/-0.178	-0.329 */-0.285	0.195/0.134
Eyelid vascularity [‡]	-0.274 */ -0.357 *	-0.340 */-0.278	0.116/0.047
Corneal sensitivity			
Detection threshold [‡]	0.092/0.073	-0.118/-0.056	-0.048/-0.013
Pain threshold [‡]	-0.123/-0.147	-0.322 */-0.268	0.071/0.005
Pain minus detection threshold [‡]	-0.162/ -0.290 *	-0.303/ -0.310 *	0.092/0.111

NRS=numerical rating scale, average ocular pain intensity, 1 week recall; NPSI-Eye=neuropathic pain symptom inventory modified for the eye;

* p value <0.05;

[‡] Analysis performed on value from right eye as functional slit lamp imaging was performed on right eye.

Table 3

Correlations between change in bulbar conjunctival microvasculature velocity and DE symptoms (including ocular pain) and signs

Continuous variables	Change in Velocity Pearson r/Spearman rho
DE symptoms	
Dry eye questionnaire 5	-0.004/-0.032
Ocular surface disease index	0.073/0.082
Ocular pain	
NRS	-0.107/-0.115
NPSI-Eye total	-0.216/-0.161
Burning spontaneous pain	-0.204/-0.183
Wind hyperalgesia	-0.268* /-0.224
Light allodynia	-0.170/-0.151
Ocular signs	
Osmolarity †	-0.172/-0.251
Tear break up time †	-0.062/-0.078
Corneal staining †	-0.102/-0.088
Schirmer's test †	0.046/0.062
Meibum quality †	-0.153/-0.125
Eyelid vascularity †	-0.132/-0.076
Corneal sensitivity	
Detection threshold †	-0.003/-0.076
Pain threshold †	-0.070/-0.061
Pain minus detection threshold †	-0.072/-0.068

NRS=numerical rating scale, average ocular pain intensity, 1 week recall; NPSI-Eye=neuropathic pain symptom inventory modified for the eye;

* p value <0.05;

† Analysis performed on value from right eye as functional slit lamp imaging was performed on right eye.